Studies of the underlying event and particle production with the ATLAS detector

James Robinson[1], on behalf of the ATLAS Collaboration

[1]Deutsches Elektronen-Synchrotron, Notkestraße 85, 22607 Hamburg, Germany

February 5, 2016

ATL-PHYS-PROC-2016-024
05 February 2016

1 Introduction

Studies of underlying event and particle production allow tuning and validation of models while helping describe pile-up and soft backgrounds to other processes. Such measurements in ATLAS [1] at the LHC use the inner tracking detectors, sensitive to charged particles with transverse momentum $p_{\mathrm{T}} > 100$ MeV and pseudorapidity $|\eta| < 2.5$, and the electromagnetic and hadronic calorimeters, sensitive to electrons, photons and hadrons that have transverse energy E_{T} greater than a few hundred MeV and $|\eta| < 4.9$. Often "Minimum Bias" events are used: inclusive collisions triggered by scintillators located at $2.1 < |\eta| < 4.9$.

2 Underlying event

Underlying event (UE) is any hadronic activity not associated with the hard scatter; an unavoidable background to collisions. UE is modelled with multiple parton interactions (MPI), initial- and final-state QCD radiation and colour-reconnection to the beam remnants. A reference object is identified in each event, such as the highest-p_{T} jet, track or Z-boson. For each particle, the azimuthal distance to the reference, $\Delta\phi$, is used to assign it to one of several regions: "towards" ($|\Delta\phi| \leq \pi/3$), "away" ($|\Delta\phi| \geq 2\pi/3$) and "transverse" ($\pi/3 < |\Delta\phi| \leq 2\pi/3$); "trans-max" and "trans-min" are subdivisions of the transverse region. UE is characterised in each region using calorimeter deposits and charged tracks.

Using a leading jet reference [2], the differential p_{T} sum of charged particles is shown for inclusive (Fig. 1a) and exclusive events (Fig. 1b). The roughly flat trans-min activity shows UE can be treated as constant at hard scales. Inclusively, activity increases in the trans-max region, showing colour connection to the jets. For exclusive events, vetoing extra jets lessens sensitivity to perturbative QCD. Another measurement at 7 TeV used a Z-boson as the reference [3], for which the towards region has a smaller amount of hard QCD activity. UE is compared for different reference objects in Fig. 2a; agreement between jet and Z-boson references supports the model of

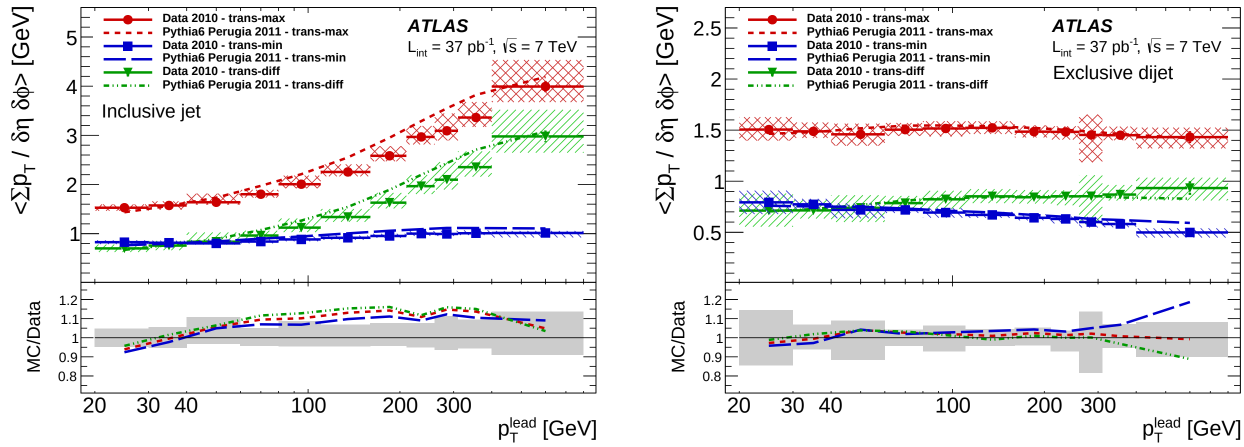

(a) Inclusive: ≥ 1 jet

(b) Exclusive: exactly two jets

Figure 1: Average scalar p_{T} sum of charged particles using a highest-p_{T} jet reference object [2].

universal MPI, as does Fig. 2a showing 13 TeV data [4]. In all cases the data are used to constrain state-of-the-art theoretical predictions.

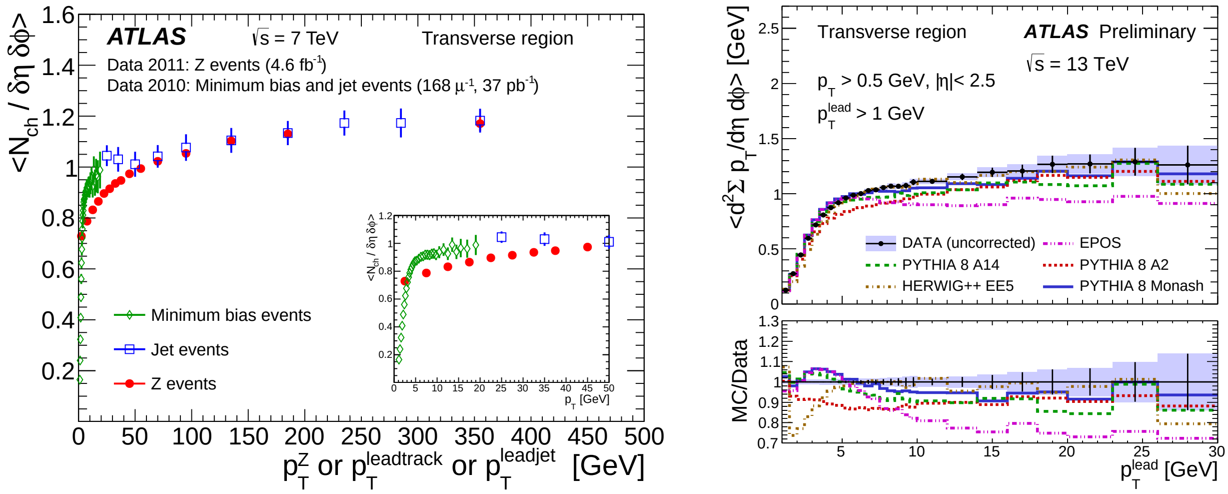

(a) Charged particle density as a function of reference object p_{T}

(b) Scalar transverse momentum density at 13 TeV with reference to the leading track

Figure 2: UE measurements using track, jet and Z-boson reference objects [3, 4].

3 Diffractive dijet production with rapidity gaps

Diffractive dijet production is analysed in terms of $\Delta\eta^{F}$, the largest forward pseudorapidity region devoid of hadronic activity and of $\tilde{\xi}$, an estimator of the fractional momentum loss in single diffractive dissociation [5]. Differential cross-sections (Fig. 3) show the non-diffractive component dominates at low $\Delta\eta^F$, but diffractive components are significant at higher $\Delta\eta^F$ and low $\tilde{\xi}$.

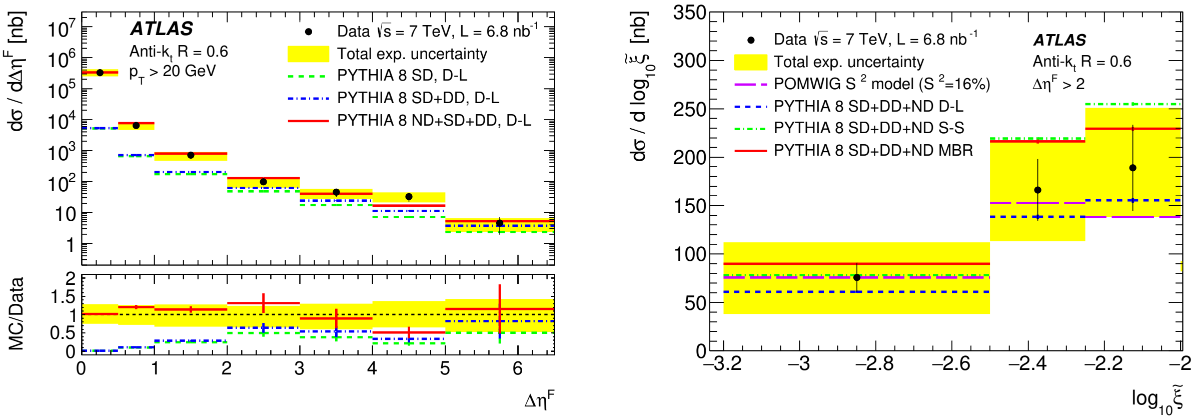

(a) As a function of $\Delta\eta^F$ (b) As a function of $\tilde{\xi}$

Figure 3: Diffractive dijet cross-sections [5].

4 Exclusive photoproduction of dileptons

The cross-section of exclusive $\gamma\gamma \to l^+l^-$ production was measured using 7 TeV data [6]. For electron or muon pairs passing a strict selection, the fiducial cross-section is extracted by fitting the dilepton acoplanarity distribution, shown in Fig. 4a. When the Equivalent Photon Approximation (EPA), which corrects for the finite proton size, is taken into account then the extracted cross-sections are found to be consistent with theoretical expectations, shown in Fig. 4b.

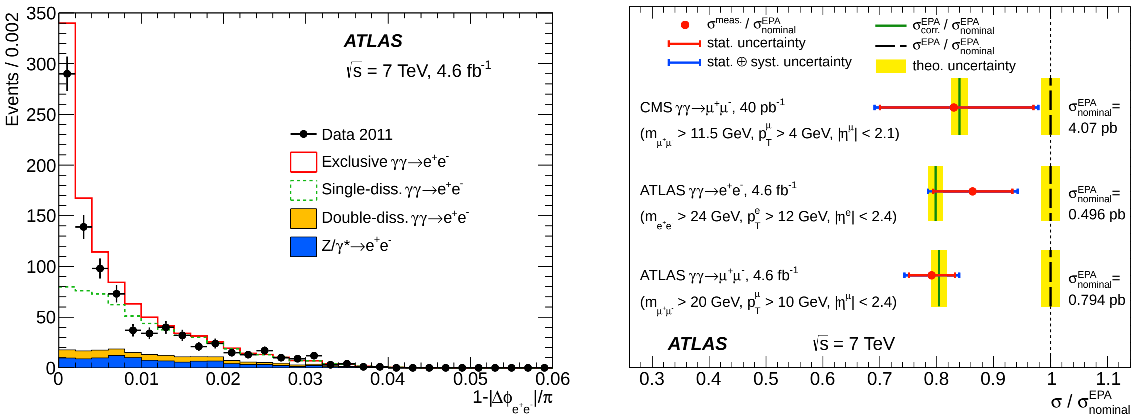

(a) Template fit to acoplanarity distribution (b) EPA-corrected cross-section

Figure 4: Extraction of single dissociative fraction and comparison to theoretical predictions [6].

5 Transverse polarisation of Λ and $\bar{\Lambda}$ hyperons

The transverse polarisation of Λ and $\bar{\Lambda}$ hyperons was measured as a function of Feynman x_F [7]. Large polarisation of Λ hyperons was observed by previous experiments, while $\bar{\Lambda}$ was consistently compatible with zero. Fig. 5a shows no significant dependence on x_F, and compatibility with zero in both cases. Fig. 5b demonstrates that the ATLAS results are compatible with an extrapolation from fixed-target experiments to the x_F range accessible in this measurement.

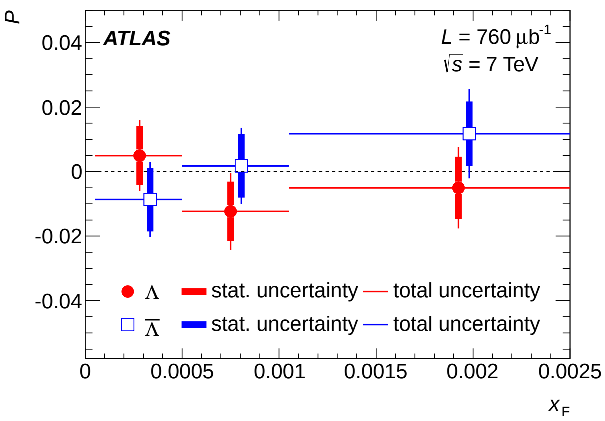

(a) Extracted polarisations for Λ and $\bar{\Lambda}$

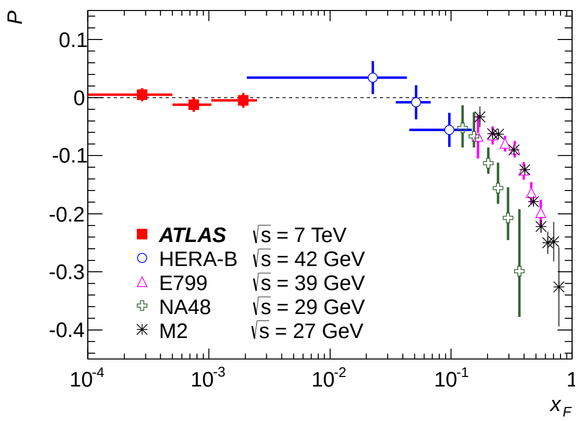

(b) ATLAS measurement compared to measurements from lower centre-of-mass energy experiments

Figure 5: Extracted $\Lambda/\bar{\Lambda}$ polarisations as a function of x_F; comparison to other measurements [7].

6 Conclusion

The ATLAS collaboration has measured underlying event with different references, diffractive dijet and dilepton production and Λ polarisation. Such measurements are helpful for the development and tuning of models of soft particle production.

References

[1] ATLAS Collaboration, *JINST*, **3**(2008), S08003.

[2] ATLAS Collaboration, *Eur. Phys. J.*, **C74**(2014), 2965, `1406.0392`.

[3] ATLAS Collaboration, *Eur. Phys. J.*, **C74**(2014), 3195, `1409.3433`.

[4] ATLAS Collaboration, Technical Report ATL-PHYS-PUB-2015-019, 2015.

[5] ATLAS Collaboration, *Phys. Lett.*, **B754**(2016), 214, `1511.00502`.

[6] ATLAS Collaboration, *Phys. Lett.*, **B749**(2015), 242, `1506.07098`.

[7] ATLAS Collaboration, *Phys. Rev.*, **D91**(2015) (3), 032004, `1412.1692`.